The Unimolecular Chemistry of the 1,4-Diradical $\cdot CH_2CH_2OCH_2\cdot$ in the Gas Phase. Comparison to the Distonic Radical Ions $\cdot CH_2CH_2OCH_2^+$ and $^-CH_2CH_2OCH_2\cdot$

Michael J. Polce and Chrys Wesdemiotis*

Contribution from the Department of Chemistry, The University of Akron, Akron, Ohio 44325-3601

Received May 26, 1992. Revised Manuscript Received May 3, 1993®

Abstract: The 1,4-diradical $\cdot CH_2CH_2OCH_2\cdot$ (**1**), which represents a ring-opened isomer of oxetane (**2**), is investigated by neutralization–reionization mass spectrometry (NRMS). **1** is produced in the gas phase by neutralization of the stable distonic radical cation $\cdot CH_2CH_2OCH_2^+$ ($\mathbf{1}^{\cdot+}$) and characterized by subsequent reionization into cations ($^+NR^+$) and anions ($^+NR^-$). Within the microsecond time window of the NRMS experiments, diradical **1** dissociates to $CH_2{=}CH_2$ + $O{=}CH_2$. A small fraction of the diradical survives undissociated, however. This fraction undergoes neither ring closure to **2** nor 1,4-hydrogen rearrangement to the carbene CH_3CH_2OCH (**3**). Thus, the barriers for C—C bond formation and H-atom migration through a five-membered ring must be higher than the barrier for C—O bond fission. The simple decomposition of **1** into $CH_2{=}CH_2$ + $O{=}CH_2$ is in sharp contrast to the unimolecular reactions of the distonic ion $\mathbf{1}^{\cdot+}$, which at threshold dissociates largely via complicated rearrangements yielding $CH_3CH_2C{\equiv}O^+$ + $\cdot H$, $CH_3C{\equiv}O^+$ + $\cdot CH_3$, and $C_2H_6^{\cdot+}$ + CO. The $^+NR^-$ data also show that **1** can form a stable molecular anion while the closed-shell isomer **2** does not.

Diradicals are the proposed intermediates in numerous thermal and photochemical reactions, including stereoisomerization, polymerization, and synthesis of ketones and alcohols,[1,2] yet many simple diradicals have escaped direct experimental characterization due to their unusually high reactivity. In sharp contrast to the neutral diradicals, their molecular cations can be surprisingly stable and readily available in the mass spectrometer through rearrangement fragmentations of larger ions (eq 1) or ion–molecule reactions.[3,4] The cationized diradicals have been called *distonic* radical cations by Radom et al.[3] to emphasize that their radical and charge sites are *distant* from each other.

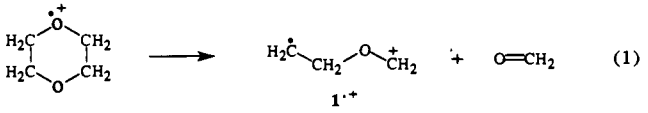

(1)

Distonic ions can serve as precursors for the synthesis of gaseous diradicals in neutralization–reionization mass spectrometry (NRMS) experiments.[5] With this technique, neutral molecules are formed in the gas phase by neutralization from the corresponding ions[6] and their unimolecular chemistry is probed by reionization. NRMS has led to new information on the stabilities and reactions of various unconventional neutrals,[7] including hypervalent species,[8a] carbenes,[8b,c] and some 1,3-diradicals.[8c–e,9] The characterization of $\cdot CH_2CH_2CH_2CH(OH)\cdot$, the simplest Norrish-type II diradical, has been reported recently.[10]

In this study, NRMS is used to provide first experimental data on the stability of the 1,4-diradical **1** and on its tendencies toward ring closure and rearrangement. **1** has been postulated as an intermediate in the thermal decomposition of oxetane (**2**). On the basis of kinetic studies and RRKM calculations, Zalotai et al.[11] proposed that pyrolysis of **2** proceeds via ring opening to **1** or to $\cdot CH_2CH_2CH_2O\cdot$ (**1′**), which then decays into $CH_2{=}CH_2$ + $O{=}CH_2$. The overall activation energies for decomposition via **2** → **1** and **2** → **1′** were found to be ~260 and 262 kJ mol^{-1}, respectively.[11]

1's precursor, the $C_3H_6O^{\cdot+}$ distonic radical ion formed after $CH_2{=}O$ loss from ionized 1,4-dioxane (eq 1), has thoroughly been studied by theory and experiment. An early investigation by McLafferty et al.[12] reported that the high-energy collisionally activated dissociation (CAD)[13] spectra of $\mathbf{1}^{\cdot+}$ and $\mathbf{2}^{\cdot+}$ were very similar. Later, high-level MO calculations of Radom et al. predicted, however, that the distonic ion $\mathbf{1}^{\cdot+}$ should be a unique, stable $C_3H_6O^{\cdot+}$ isomer.[14] This has indeed been confirmed by its distinctive ion–molecule reactions,[15] heat of formation,[16] and

* Abstract published in *Advance ACS Abstracts*, October 1, 1993.

(1) (a) Wentrup, C. *Reactive Molecules: The Neutral Reactive Intermediates in Organic Chemistry*; Wiley Interscience: New York, 1984; pp 128–161. (b) Borden, W. T., Ed. *Diradicals*; Wiley: New York, 1982.

(2) (a) Wagner, P. J. *Acc. Chem. Res.* **1989**, *22*, 83–91. (b) Doubleday, C., Jr.; Turro, N. J.; Wang, L. *Ibid.* **1989**, *22*, 199–205.

(3) Yates, B. F.; Bouma, W. J.; Radom, L. *J. Am. Chem. Soc.* **1984**, *106*, 5805–5808.

(4) Hammerum, S. *Mass Spectrom. Rev.* **1988**, *7*, 123–202.

(5) (a) Wesdemiotis, C.; McLafferty, F. W. *Chem. Rev.* **1987**, *87*, 485–500. (b) Terlouw, J. K.; Schwarz, H. *Angew. Chem., Int. Ed. Engl.* **1987**, *26*, 808–815. (c) Holmes, J. L. *Mass Spectrom. Rev.* **1989**, *8*, 513–539.

(6) Gellene, G. I.; Porter, R. F. *Acc. Chem. Res.* **1983**, *16*, 200–207.

(7) McLafferty, F. W. *Science* **1990**, *247*, 925–929.

(8) (a) Wesdemiotis, C.; Feng, R.; Danis, P. O.; Williams, E. R.; McLafferty, F. W. *J. Am. Chem. Soc.* **1986**, *108*, 5847–5853. (b) Wesdemiotis, C.; McLafferty, F. W. *Ibid.* **1987**, *109*, 4760–4761. (c) Wesdemiotis, C.; Leyh, B.; Fura, A.; McLafferty, F. W. *Ibid.* **1990**, *112*, 8655–8660. (d) Turecek, F.; Drinkwater, D. E.; McLafferty, F. W. *Ibid.* **1991**, *113*, 5950–5958. (e) Srinivas, R.; Böhme, D. K.; Hrusák, J.; Schröder, D.; Schwarz, H. *Ibid.* **1992**, *114*, 1939–1942.

(9) An alternative route to diradicals, namely via dissociation of anions, has been reported recently. See: Wenthold, P. G.; Paulino, J. A.; Squires, R. S. *J. Am. Chem. Soc.* **1991**, *113*, 7414–7415.

(10) Polce, M. J.; Cordero, M. M.; Wesdemiotis, C.; Bott, P. A. *Int. J. Mass Spectrom. Ion Processes* **1991**, *113*, 35–58.

(11) Zalotai, L.; Hunyadi-Zoltán, Z.; Bérces, T.; Márta, F. *Int. J. Chem. Kinet.* **1983**, *15*, 505–519.

(12) Van de Sande, C. C.; McLafferty, F. W. *J. Am. Chem. Soc.* **1975**, *97*, 4617–4620.

(13) (a) McLafferty, F. W.; Bente, P. F., III; Kornfeld, R.; Tsai, S.-C.; Howe, I. *J. Am. Chem. Soc.* **1973**, *95*, 2120–2129. (b) Busch, K. L.; Glish, G. L.; McLuckey, S. A. *Mass Spectrometry/Mass Spectrometry*; VCH Publishers, Inc.: New York, 1988.

(14) Bouma, W. J.; MacLeod, J. K.; Radom, L. *J. Am. Chem. Soc.* **1980**, *102*, 2246–2252.

(15) Baumann, B. C.; MacLeod, J. K.; Radom, L. *J. Am. Chem. Soc.* **1980**, *102*, 7927–7928.

0002-7863/93/1515-10849$04.00/0

energy-resolved CAD spectra.[17] The bimolecular chemistry of ions $1^{\bullet+}$ and $2^{\bullet+}$ has been thoroughly explored[18-21] and was recently reviewed by Kenttämaa et al.[22] In contrast, their unimolecular chemistry has only been addressed briefly.[12,17,19] This study ascertains the unimolecular dissociations of $1^{\bullet+}$ and $2^{\bullet+}$ and compares them to those of the corresponding neutrals. First data are also presented on the stabilities and reactivities of the radical anions $1^{\bullet-}$ and $2^{\bullet-}$, which have not yet been documented experimentally.

Experimental Section

Measurements were made with a modified VG AutoSpec tandem mass spectrometer, which has been described in detail.[10] This trisector E_1BE_2 instrument is equipped with three collision cells, one (Cls-1) in the first field-free region (FFR-1) preceding the first electrostatic analyzer and two (Cls-2 and Cls-3) in the third field-free region (FFR-3) located between E_1B and E_2.

Unless noted otherwise, the desired precursor cation was produced by electron ionization of the appropriate sample at 70 eV, accelerated to 8 keV, and mass-selected by E_1B. In neutralization–reionization (NR) experiments, the selected radical cation was reduced in Cls-2 by collisions with Xe. After removal of the unneutralized fraction by electrostatic deflection (indicated by /), the remaining beam of fast neutrals was collisionally reoxidized by O_2 in Cls-3; the newly formed product cations were mass-analyzed through E_2 and recorded in the $^+NR^+$ Xe/O_2 spectrum. The pressures adjusted with Xe and O_2 reduced the parent ion beam intensity by 20% in each collision cell (80% transmittance), corresponding to ~single collision conditions with each target.[23] The superscripts indicate the charges of the precursor and the ultimate product ions.

$^+NR^-$ Xe/Xe spectra can be measured similarly by using Xe in both collision cells. Alternatively, neutralization and anionization can be combined in the same collision cell (Cls-3)[24] to obtain $^+NR^-$ Xe (50% transmittance) spectra. These latter spectra contain all negative ions formed from the selected precursor cation during multiple collisions with Xe. It has been shown for polyatomic cations that under such multicollision conditions, the anions are formed by sequential addition of e^-, not simultaneous attachment of $2e^-$ and cogeneration of Xe^{2+}.[25,26] We confirmed this for the allyl alcohol cation, whose $^+NR^-$ Xe and $^+NR^-$ Xe/Xe spectra are very similar.[27] By combining the neutralization and anionization collisions in the same cell, the signal yield increases by ~1.5 orders of magnitude.

Metastable ion (MI) and CAD spectra were acquired with no collision gas and O_2 in Cls-3 (80% transmittance), respectively. The acquisition of MI spectra in FFR-1 was performed using linked-scan techniques.[13b] For MS/MS/MS spectra, the precursor ion was produced in FFR-1 and subjected to MI and CAD experiments in FFR-3. The MI, CAD, $^+NR^+$ and $^+NR^-$ spectra were recorded with the slits completely open for maximum sensitivity. Under these conditions, the main beam width at half-height ($W_{0.5}$) is 14–15 V for 8 keV precursor ions. Kinetic energy releases ($T_{0.5}$) were measured at higher energy resolution, with $W_{0.5}$ (main beam) being ~6 V. The reported values are corrected for the width of the main beam and were calculated according to established procedures.[28,29]

All samples are commercially available and were introduced into the instrument without further purification. In the CAD spectra, the relative product ion abundances were not altered outside experimental error if the target pressure was varied from 80 to 50% transmittance. In sharp contrast, the $^+NR^+$ and $^+NR^-$ spectra were found to be particularly sensitive to variations in the pressures of the gas targets. Therefore, the NR spectra compared to each other were measured sequentially under identical experimental conditions and combine multiple averaged scans (reproducibility better than ±10% for $^+NR^+$ and ±20% for $^+NR^-$).

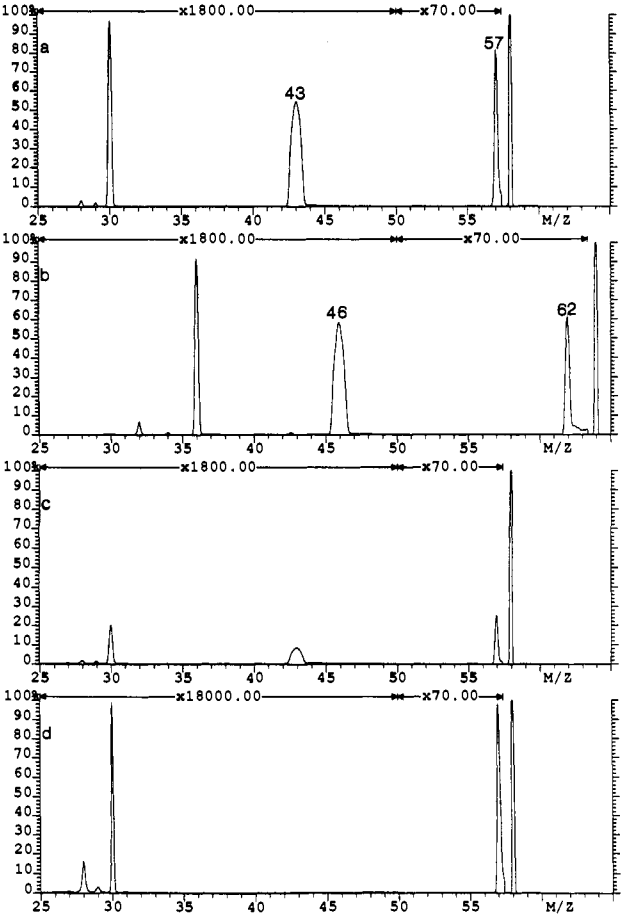

Figure 1. MI spectra of $C_3H_6O^{\bullet+}$ cations decomposing in FFR-3: (a) $1^{\bullet+}$ at 70 eV, (b) d_6-$1^{\bullet+}$ at 70 eV, (c) $1^{\bullet+}$ at 15 eV, and (d) $2^{\bullet+}$ at 70 eV.

Results and Discussion

Precursor Radical Cations. The incipient distonic radical cation $1^{\bullet+}$ and its ring-closed isomer $2^{\bullet+}$ (ionized oxetane) are formed upon electron ionization of 1,4-dioxane (eq 1) and oxetane, respectively. Before these $C_3H_6O^{\bullet+}$ ions can be used for the synthesis of the corresponding neutrals, it must be established that they still have their original structures when they enter the neutralization region. Ions $1^{\bullet+}$ and $2^{\bullet+}$ with kinetic energies in the eV range have been distinguished by low-energy CAD[17] and ion–molecule reactions.[18-22] However, the detailed unimolecular chemistry of multi-keV ions, which are employed in neutralization–reionization experiments, has not been elucidated yet.[12,17,19]

MI Spectra. According to Figure 1, the major dissociation channel (>95%) of metastable ions $1^{\bullet+}$ and $2^{\bullet+}$ in the third field-free region of the instrument is H• loss to form $C_3H_5O^+$. This reaction gives rise to Gaussian peaks with the same kinetic energy release for both ions ($T_{0.5}$ = 369 meV). The $C_3H_5O^+$ product

(16) Fraser-Monterio, M. L.; Fraser-Monteiro, L.; Butler, J. J.; Baer, T.; Hass, J. R. *J. Chem. Phys.* **1982**, *86*, 739–747.
(17) Verma, S.; Ciupek, J. D.; Cooks, R. G. *Int. J. Mass Spectrom. Ion Processes* **1984**, *62*, 219–225.
(18) Bouchoux, G. *Mass Spectrom. Rev.* **1988**, *7*, 1–39, 203–255.
(19) Wittneben, D.; Grützmacher, H.-F. *Int. J. Mass Spectrom. Ion Processes* **1990**, *100*, 545–563.
(20) (a) Kiminkinen, L. K. M.; Stirk, K. G.; Kenttämaa, H. I. *J. Am. Chem. Soc.* **1992**, *114*, 2027–2031. (b) Stirk, K. M.; Orlowski, J. C.; Leeck, D. T.; Kenttämaa, H. I. *Ibid.* **1992**, *114*, 8604–8606.
(21) Audier, H. E.; Milliet, A.; Leblanc, D.; Morton, T. H. *J. Am. Chem. Soc.* **1992**, *114*, 2020–2027.
(22) Stirk, K. M.; Kiminkinen, M.; Kenttämaa, H. I. *Chem. Rev.* **1992**, *92*, 1649–1665.
(23) Todd, P. J.; McLafferty, F. W. *Int. J. Mass Spectrom. Ion Phys.* **1981**, *38*, 371–378.
(24) (a) Feng, R.; Wesdemiotis, C.; McLafferty, F. W. *J. Am. Chem. Soc.* **1987**, *109*, 6521–6522. (b) McLafferty, F. W.; Wesdemiotis, C. *Org. Mass Spectrom.* **1989**, *24*, 663–668.
(25) Leyh, B.; Wankenne, H. *Int. J. Mass Spectrom. Ion Processes* **1991**, *107*, 453–474.
(26) (a) Griffiths, W. J.; Harris, F. M.; Barton, J. D. *Rapid Commun. Mass Spectrom.* **1989**, *3*, 283–285. (b) Griffiths, W. J.; Harris, F. M.; Reid, C. J.; Ballantine, J. A. *Org. Mass Spectrom.* **1989**, *24*, 849–850.
(27) Polce, M. J.; Wiedmann, F. A.; Wesdemiotis, C., manuscript in preparation.
(28) Cooks, R. G.; Beynon, J. H.; Caprioli, R. M.; Lester, G. R. *Metastable Ions*; Elsevier: Amsterdam, 1973.
(29) Holmes, J. L. *Org. Mass Spectrom.* **1985**, *20*, 169–183.

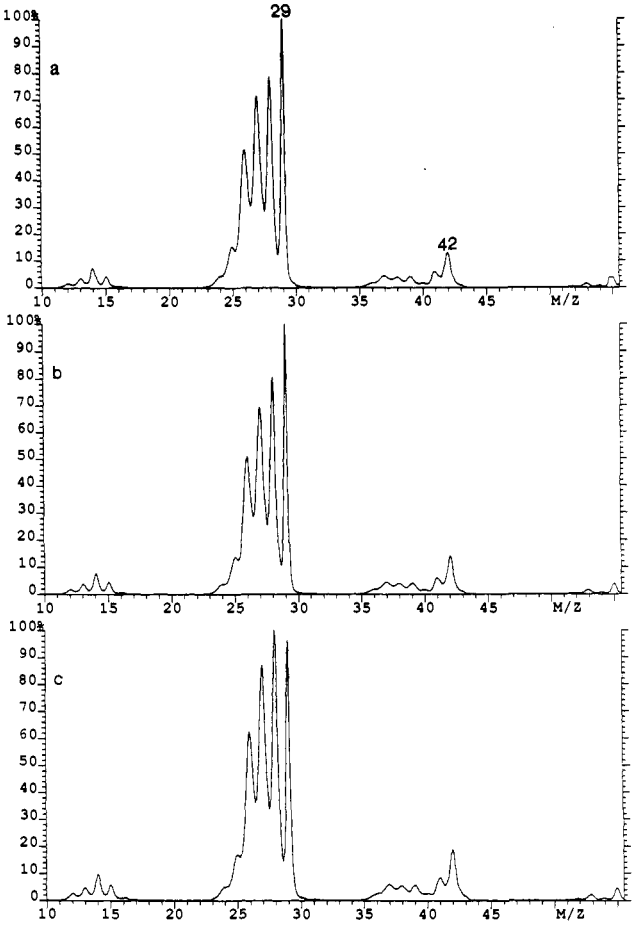

Figure 2. CAD spectra (acquired in FFR-3) of $C_3H_5O^+$ cations produced in FFR-1 from metastable (a) $\mathbf{1}^{\bullet+}$, (b) $\mathbf{2}^{\bullet+}$, and (c) $CH_3CH_2CH{=}O^{\bullet+}$. The corresponding MI spectra contain fragments at m/z 56 and 29.

Table I. Decomposition Products of Metastable Ions $\mathbf{1}^{\bullet+}$ and $\mathbf{2}^{\bullet+}$[a]

m/z	products[b]	ΔH°_f(kJ mol^{-1})[c]
57	$CH_3CH_2C{\equiv}O^+ + \cdot H$	591 + 218 = 809
	$\{CH_2{=}CHOCH_2^+ + \cdot H$	751[d] + 218 = 969$\}$
	$\{CH_2CH{=}O^+CH_2 + \cdot H$	759[d] + 218 = 977$\}$
43	$CH_3C{\equiv}O^+ + \cdot CH_3$	653 + 146 = 799
30	$CH_3CH_3^{\bullet+} + CO$	1028 + (−111) = 917
	$\{CH_2{=}O^{\bullet+} + CH_2{=}CH_2$	941 + 52 = 993$\}$
29	$CH_3CH_2^+ + HCO\cdot$	902 + 45 = 947
	$HCO^+ + CH_3CH_2\cdot$	826 + 118 = 944
28	$CH_2{=}CH_2^{\bullet+} + O{=}CH_2$	1066 + (−109) = 957
	$\{CO^{\bullet+} + CH_3CH_3$	1242 + (−84) = 1158$\}$

[a] The ΔH°_f values of ions $\mathbf{1}^+$ and $\mathbf{2}^+$ are 828 and 852 kJ mol^{-1}, respectively.[16,32] [b] Not observed products are shown in brackets. [c] From ref 32. [d] From ref 19.

has the structure of the propanoyl cation $CH_3CH_2CO^+$. This was determined by MS/MS/MS: $C_3H_5O^+$ ions were generated from metastable $\mathbf{1}^{\bullet+}$ or $\mathbf{2}^{\bullet+}$ in FFR-1 and their CAD spectra acquired in FFR-3. These MS/MS/MS spectra are identical within experimental error to the reference CAD spectrum of $CH_3CH_2CO^+$, produced similarly from metastable propanal ions (Figure 2). Consequently, loss of H• from $\mathbf{1}^{\bullet+}$ and $\mathbf{2}^{\bullet+}$ must be accompanied by complicated rearrangements and does not produce $CH_2{=}CHOCH_2^+$ or the oxetanyl cation (Table I), as assumed previously.[19]

Profound differences between metastable ions $\mathbf{1}^{\bullet+}$ and $\mathbf{2}^{\bullet+}$ are observed for the less abundant decompositions leading to m/z 43 and 30 (Figure 1a vs Figure 1d). Elimination of $\cdot CH_3$ to yield $C_2H_3O^+$ (m/z 43) is observed only for ion $\mathbf{1}^{\bullet+}$ and leads to a broad signal with no discernible dished or flat top ($T_{0.5}$ = 479 meV). On the other hand, both isomers contain fragment ions of m/z 30 (Gaussian shape) in their MI spectra. MS/MS/MS on such fragments produced in FFR-1 shows that they can lose up to six H atoms and, hence, indicate the composition $C_2H_6^{\bullet+}$. That the ions of m/z 30 are the result of unimolecular decay into $C_2H_6^{\bullet+}$ + CO, not $O{=}CH_2^{\bullet+} + C_2H_4$, is also evident from the MI spectrum of d_6-$\mathbf{1}^{\bullet+}$ (Figure 1b), in which the corresponding peak is shifted by 6 units to m/z 36. Grützmacher et al. came to a similar conclusion from the study of partially deuterated isotopomers of $\mathbf{1}^{\bullet+}$.[19] It is noteworthy that the kinetic energy releases for the formation of $C_2H_6^{\bullet+}$ from $\mathbf{1}^{\bullet+}$ and $\mathbf{2}^{\bullet+}$ are substantially different, with $T_{0.5}$ values of 33 meV for $\mathbf{1}^{\bullet+}$ but only 7.6 meV for $\mathbf{2}^{\bullet+}$. This result reveals that distinct paths are followed by $\mathbf{1}^{\bullet+}$ and $\mathbf{2}^{\bullet+}$ during CO loss.[28]

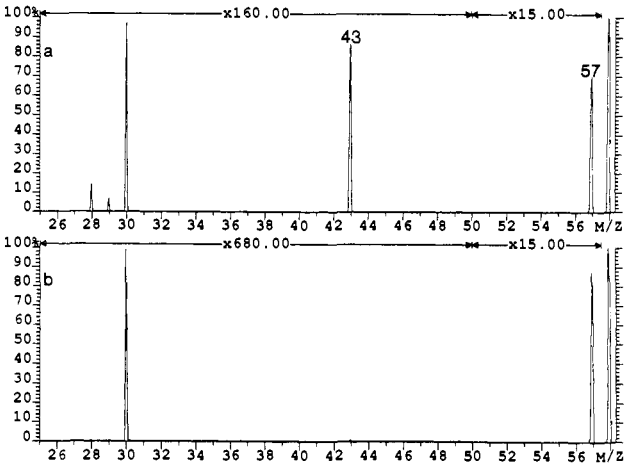

Figure 3. MI spectra of cations (a) $\mathbf{1}^{\bullet+}$ and (b) $\mathbf{2}^{\bullet+}$, decomposing in FFR-1 (70 eV).

Finally, both $\mathbf{1}^{\bullet+}$ and $\mathbf{2}^{\bullet+}$ show weak fragments at m/z 28 and 29. Since the former quantitatively shifts to m/z 32 in the spectrum of d_6-$\mathbf{1}^{\bullet+}$, it represents $C_2H_4^{\bullet+}$, not $CO^{\bullet+}$. The latter partly moves to m/z 34 (57%) and partly to m/z 30 (43%), consistent with being a mixture of $C_2H_5^+$ and HCO^+. $C_2H_4^{\bullet+}$ and $C_2H_5^+/HCO^+$ are extremely weak for $\mathbf{2}^{\bullet+}$ (<0.1% of MI base peak) and could, therefore, originate in part from CAD with the background gases, as they are formed with high yields upon CAD (*vide infra*). The dissociation limits for the reactions of metastable $\mathbf{1}^{\bullet+}$ and $\mathbf{2}^{\bullet+}$ are summarized in Table I. The eliminations of H• and $\cdot CH_3$ are exothermic and must, therefore, be associated with sizable activation energies, the presence of which is also indicated by the corresponding large kinetic energy releases.

The average lifetime of metastable $C_3H_6O^{\bullet+}$ ions decomposing in FFR-3 is ~10.5 μs. Ions with shorter lifetimes (~0.85 μs) and, thus, higher average internal energies are probed in FFR-1; they show parallel characteristics (Figure 3 *vis à vis* Figure 1). Lowering the internal energy of ions $\mathbf{1}^{\bullet+}$ and $\mathbf{2}^{\bullet+}$ by forming them at 15 eV reduces the overall dissociation extent but does not affect greatly the *relative* fragment ion abundances (see, e.g., Figure 1c). This insensibility of MI spectra to changes in internal energy precludes that ions $\mathbf{1}^{\bullet+}$ and $\mathbf{2}^{\bullet+}$ consist of mixtures and is rather consistent with the presence of isomerically pure structures.[13b,29]

$\mathbf{1}^{\bullet+}$ can also be produced in FFR-1 from metastable 1,4-dioxane cations. In the MI spectrum of such metastably produced $\mathbf{1}^{\bullet+}$, $[C_3H_5O^+]$:$[\mathbf{1}^{\bullet+}]$ is ~50 times smaller than that for $\mathbf{1}^{\bullet+}$ generated in the ion source, while the other fragments are not discernable above noise level. The *average* internal energy of metastably generated $\mathbf{1}^{\bullet+}$ has been found by Baer et al. to be only 17 kJ mol^{-1}.[16,30] The critical energy needed to form $C_3H_5O^+ + \cdot H$ from $\mathbf{1}^{\bullet+}$ is, however, substantially higher judging by the large

(30) Burgers, P. C.; Holmes, J. L. *Rapid Commun. Mass Spectrom.* **1989**, *3*, 279–280.

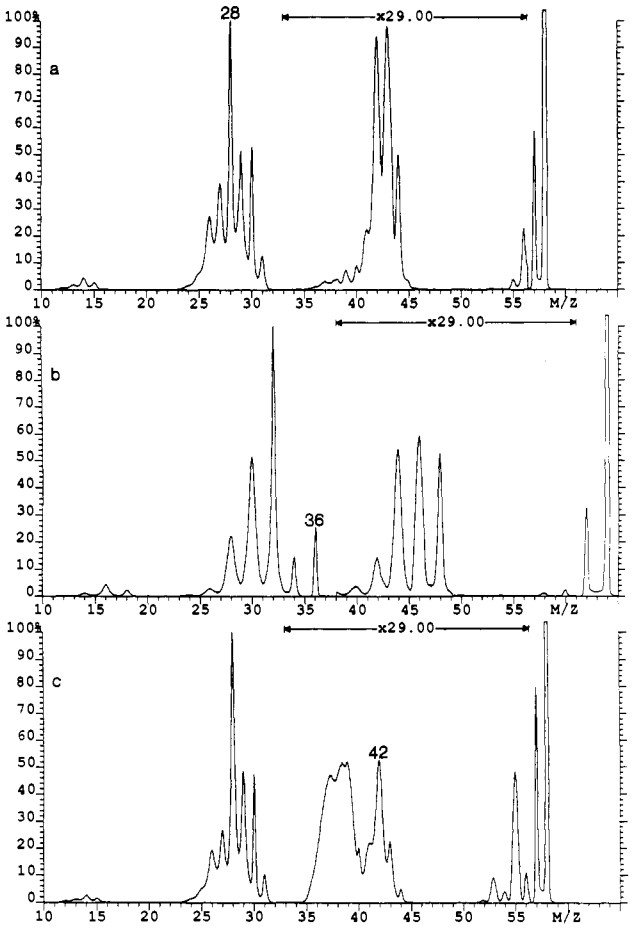

Figure 4. CAD spectra of cations (a) $1^{\bullet+}$, (b) d_6-$1^{\bullet+}$, and (c) $2^{\bullet+}$ (FFR-3).

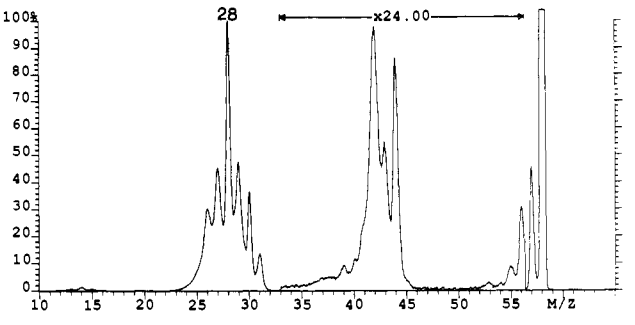

Figure 5. CAD spectrum of $1^{\bullet+}$, formed in FFR-1 from metastable 1,4-dioxane ions.

kinetic energy release associated with this reaction (36 kJ mol^{-1}, *vide supra*). Obviously, the internal energy of metastably produced $1^{\bullet+}$ is not sufficient for its spontaneous fragmentation, and the very small $C_3H_5O^+$ fragment observed most likely results from CAD with residual gases.

CAD Spectra. Upon CAD, additional reaction pathways become available, leading to abundant fragments from m/z 24 to 31 (to m/z 36 for the deuterated ion; Figure 4). Now, $C_2H_4^{\bullet+}$, which can be formed by direct bond cleavage(s), becomes the base peak. Nevertheless, the $C_2D_6^{\bullet+}$ (m/z 36) and $C_2D_5^+$/$^+CD_2OD$ (m/z 34) products in the CAD spectrum of d_6-$1^{\bullet+}$ show that rearrangements remain favored even after collisional activation.

Precursor ions $1^{\bullet+}$ produced from metastable 1,4-dioxane$^{\bullet+}$ in FFR-1 and, hence, of lower average internal energy than ions $1^{\bullet+}$ formed in the ion source give rise to the CAD spectrum of Figure 5. Lower energy content reduces the overall fragment ion yield (Σ[fragments$^+$]:[$1^{\bullet+}$]) by ~50%. At the same time, the *relative* abundances of $C_2H_6^{\bullet+}$ (m/z 30, CO loss), $C_2H_3O^+$ (m/z 43, $\cdot CH_3$ loss), and $C_3H_5O^+$ (m/z 57, $\cdot H$ loss) decrease, while that of $C_2H_4O^{\bullet+}$ (m/z 44, CH_2 loss) increases (viz. Figure 5 vs Figure 4a). The first three ions are the main MI products of $1^{\bullet+}$ and originate via low-energy rearrangements, which are known to be particularly susceptible to internal energy variations.[13,29] However, the energy dependence of the CH_2 elimination, a process of high critical energy (*vide infra*), is surprising. The possibility of the CH_2 loss involving rearrangement was examined by MS/MS/MS of the $C_2H_4O^{\bullet+}$ fragment produced in FFR-1 by CAD of $1^{\bullet+}$ and $2^{\bullet+}$. The CAD spectra of these $C_2H_4O^{\bullet+}$ fragment ions are identical to that of authentic $CH_2OCH_2^{\bullet+}$ (from 1,3-dioxolane[31]). Thus, CH_2 loss from $1^{\bullet+}$ is not preceded by molecular reorganizations and produces a fragment ion that agrees with the connectivity of $1^{\bullet+}$. $1^{\bullet+} \rightarrow CH_2OCH_2^{\bullet+} + CH_2$ ($\Sigma\Delta H°_f$ = 1252 kJ mol^{-1})[32] requires >3 eV more energy than the reaction giving rise to the CAD base peak, namely $1^{\bullet+} \rightarrow C_2H_4^{\bullet+} + OCH_2$ ($\Sigma\Delta H°_f$ = 957 kJ mol^{-1}).[32] Yet, the former process becomes more competitive when $1^{\bullet+}$ has lower internal energy (Figure 5 vs Figure 4a). This can be rationalized if the CH_2 loss proceeds from an excited electronic state, to which $1^{\bullet+}$ is most efficiently promoted from its ground state but which cannot readily be accessed if ion $1^{\bullet+}$ is vibrationally excited. Consistent with such a mechanism requiring electronic excitation, CH_2 loss is not observed with collisions at low kinetic energies (10–100 eV),[17] which are widely accepted to provide vibrational but not electronic excitation.[13b]

As a molecular cation, isomer $2^{\bullet+}$ cannot be prepared by a metastable decomposition in FFR-1. In this case, ions of lower average internal energies can be probed by ionizing at 15 eV instead of 70 eV. CAD of ions $2^{\bullet+}$ formed at 15 eV leads to ~50% less total fragments than CAD of $2^{\bullet+}$ generated at 70 eV. The *relative* fragment ion abundances in the CAD spectrum do not change, however, outside experimental error (spectrum at 15 eV similar to Figure 4c). Thus, internal energy variations affect isomers $1^{\bullet+}$ and $2^{\bullet+}$ differently. This result is in keeping with the low-energy CAD study of Verma et al.,[17] who monitored the abundances of selected CAD fragments from $1^{\bullet+}$ and $2^{\bullet+}$ as a function of collision energy (10–100 eV) and found that the fragment abundances for $1^{\bullet+}$ continuously changed over the entire energy range, while those for $2^{\bullet+}$ showed a different energy dependence up to ~50 eV and remained fairly constant thereafter.[17] The precise reasons for the greater energy dependence of the unimolecular reactions of cation $1^{\bullet+}$ remain unknown.

The differences between isomers $1^{\bullet+}$ and $2^{\bullet+}$ are most prominent in the region between m/z 33 and 56. For example, the abundances of $C_3H_{0-3}^+$ (m/z 36–39) are >10 times higher for ion $2^{\bullet+}$, which contains three adjacent carbons. On the other hand, CH_2 loss is ~10 times larger for the distonic ion $1^{\bullet+}$, as expected from its structure containing terminal methylene groups. Distinct also are the relative intensities of CH_3CO^+ (higher for $1^{\bullet+}$) and $C_3H_3O^+$ (m/z 55, higher for $2^{\bullet+}$). Because of these differences and the unique MI data for ions $1^{\bullet+}$ and $2^{\bullet+}$, we conclude that these two cations represent distinct $C_3H_6O^{\bullet+}$ isomers which maintain their original structures and do not freely interconvert in the microsecond time window.[29] This result is in agreement with the distinctive ion–molecule reactions of ions $1^{\bullet+}$ and $2^{\bullet+}$.[15,19-22] Having established the structures of these precursor cations, we can now proceed with the preparation and the characterization of the corresponding neutrals.

Diradical $\cdot CH_2CH_2OCH_2\cdot$ (1). Preparation of 1 by Xe Neutralization. The 1,4-diradical $\cdot CH_2CH_2OCH_2\cdot$ is a proposed intermediate of the unimolecular decay of oxetane (**2**) into $CH_2{=}CH_2 + O{=}CH_2$.[11] **1** is accessed directly by neutralization of the distonic ion $1^{\bullet+}$. After reionization into cations, dominant

(31) Buschek, J. M.; Holmes, J. L.; Terlouw, J. K. *J. Am. Chem. Soc.* **1987**, *109*, 7321–7325.

(32) Lias, S. G.; Bartmess, J. E.; Liebman, J. F.; Holmes, J. L.; Levin, R. D.; Mallard, W. G. *J. Phys. Chem. Ref. Data* **1988**, *17*, Supplement No. 1.

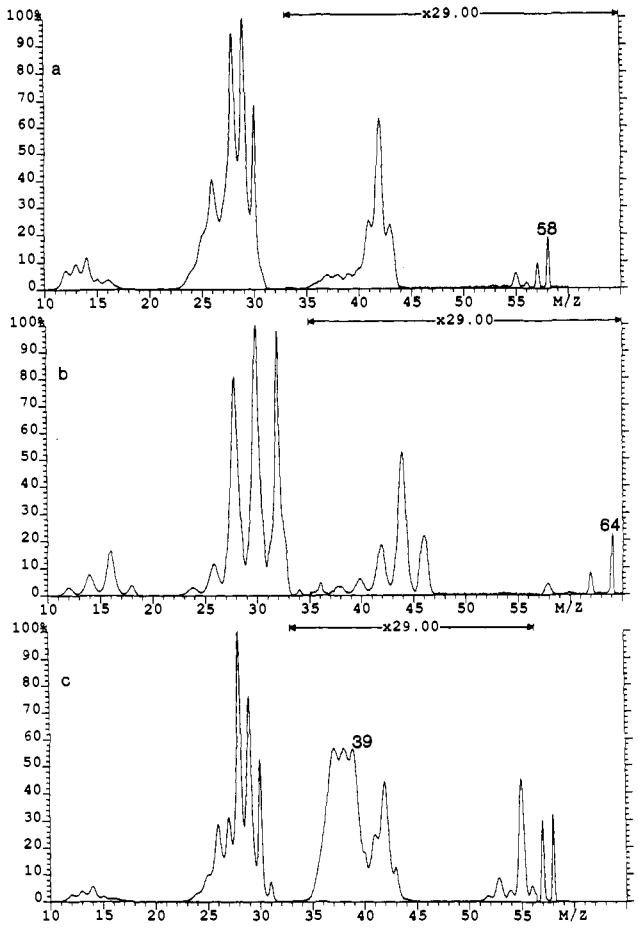

Figure 6. $^+NR^+$ Xe/O_2 spectra of cations (a) $1^{\cdot+}$, (b) d_6-$1^{\cdot+}$, and (c) $2^{\cdot+}$.

peaks are observed up to m/z 30 (Figure 6a), verifying that **1** (mass 58 Da) readily decomposes into ethylene (28 Da) and formaldehyde (30 Da). $CH_2{=}CH_2$ can contribute to m/z 12–15 and 24–28 and $O{=}CH_2$ to m/z 12–14, 16, and 28–30. Partial overlapping of these reionization products gives rise to the abundance pattern of Figure 6a. The isomer d_6-$1^{\cdot+}$ behaves similarly; its $^+NR^+$ produces abundant fragments up to m/z 32, from dissociation of d_6-**1** (64 Da) into C_2D_4 (32 Da) and $O{=}CD_2$ (32 Da). A finite part of **1** (and d_6-**1**) survives *undissociated*, however, because a measurable recovered parent ion is present in both the $^+NR^+$ *and* $^+NR^-$ (Figure 7) spectra. The identity of these recovery peaks must be established before any conclusions can be drawn on the stability of diradical **1** (*vide infra*).

The dissociation of diradical **1** into ethylene plus formaldehyde via a simple bond cleavage is in sharp contrast to the threshold fragmentations of the distonic ion $1^{\cdot+}$, which proceed after complicated isomerizations (*vide supra*). Such large differences in the unimolecular reactivities of neutrals and their molecular cations have been found for several other systems, by both experiment and theory.[5,33]

Neutralization vs CAD of $1^{\cdot+}$. Collisions with Xe effect charge exchange but can also cause CAD of precursor ion $1^{\cdot+}$ (eq 2).[34] The major neutral CAD fragment of ion $1^{\cdot+}$, $O{=}CH_2$ (eq 2a), is also formed, together with $CH_2{=}CH_2$, upon decomposition of diradical **1** (eq 2b). Both these processes yield $O{=}CH_2^{\cdot+}$ after reionization, which will overlap with any $O{=}CH_2^{\cdot+}$ originating from dissociation of the recovered $C_3H_6O^{\cdot+}$ precursor ion. The latter should, however, be very small; judging from the small

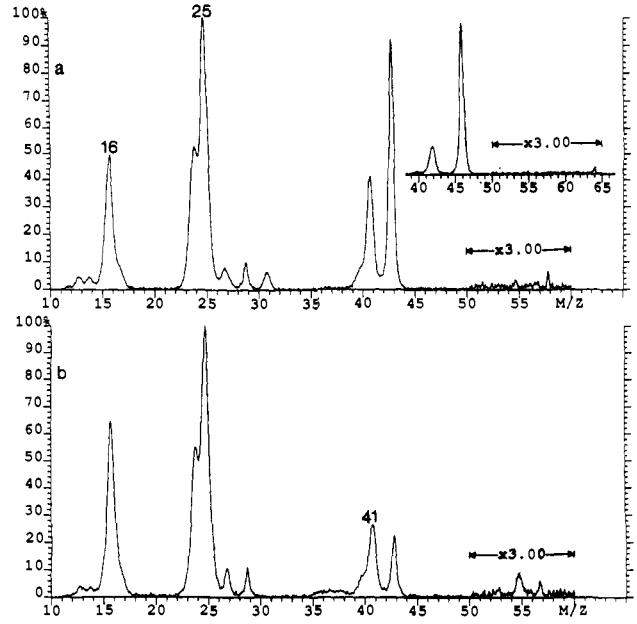

Figure 7. $^+NR^-$ Xe spectra of cations (a) $1^{\cdot+}$ and (b) $2^{\cdot+}$. The inset shows a partial $^+NR^-$ spectrum of d_6-$1^{\cdot+}$.

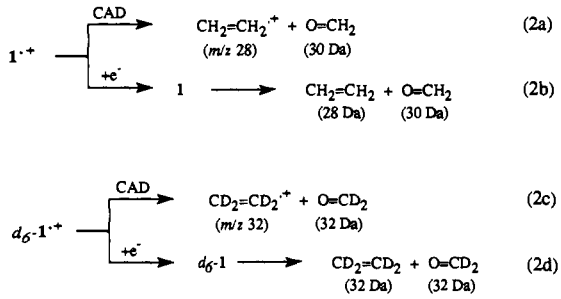

abundance of the recovery peak *and* the fragments above m/z 30, dissociation of the $C_3H_6O^{\cdot+}$ ions generated upon reionization cannot be an appreciable contributor to the intense products between m/z 12–30.

The processes of eqs 2a and 2b (or eqs 2c and 2d) can be distinguished on the basis of the kinetic energy releases with which they produce $O{=}CH_2^{\cdot+}$. It has been shown by Hop and Holmes[35] that dissociative neutralization (eqs 2b and 2d) releases more internal energy into translational energy than CAD of ions (eqs 2a and 2c). Therefore, it leads to broader signals than CAD. The extent of CAD can be maximized by choosing He or O_2 instead of Xe.[34] With O_2, the peak shapes of Figures 8a and 8b are observed for reionized $O{=}CH_2^{\cdot+}$ from $1^{\cdot+}$ and $O{=}CD_2^{\cdot+}$ from d_6-$1^{\cdot+}$, respectively. With Xe, on the other hand, composite peaks with broad bases are obtained (Figures 8c and 8d), indicating that now both mechanisms of eq 2 operate. The broad component for $CH_2{=}CH_2$, which is coproduced with $O{=}CH_2$ (eq 2b), cannot be seen due to poor resolution (viz. Figure 6a). With d_6-$1^{\cdot+}$, $CD_2{=}CD_2$ becomes isobaric with $O{=}CD_2$ (eq 2d); in this case, both neutrals can contribute to the same broad component, thus substantially increasing its relative amount (Figure 8d vs Figure 8c).[36]

Neutralization–Reionization of Ion $2^{\cdot+}$. The $^+NR^+$ and CAD spectra of ion $2^{\cdot+}$ are fairly similar (Figure 4c vs Figure 6c). The presence of the structurally characteristic fragments $C_3H_{0-3}^+$ in

(33) Burgers, P. C.; Lifshitz, C.; Ruttink, P. J. A.; Schaftenaar, G.; Terlouw, J. K. *Org. Mass Spectrom.* **1989**, *24*, 579–590.

(34) (a) Danis, P. O.; Feng, R.; McLafferty, F. W. *Anal. Chem.* **1986**, *58*, 348–354. (b) Holmes, J. L.; Mommers, A. A.; Terlouw, J. K.; Hop, C. E. C. A. *Int. J. Mass Spectrom. Ion Processes* **1986**, *68*, 249–264.

(35) Hop, C. E. C. A.; Holmes, J. L. *Int. J. Mass Spectrom. Ion Processes* **1991**, *104*, 213–216.

(36) The widths at half-height of the narrow (n) and broad (b) components of the signals in Figure 8 are as follows: (a) $W_{0.5}(n)$ = 38 V; (b) $W_{0.5}(n)$ = 43 V; (c) $W_{0.5}(n)$ = 39 V, $W_{0.5}(b)$ = 214 V; (d) $W_{0.5}(n)$ = 40 V, $W_{0.5}(b)$ = 216 V. The uncertainties are ±5 V for the narrow peaks and ±10 V for the broad peaks.

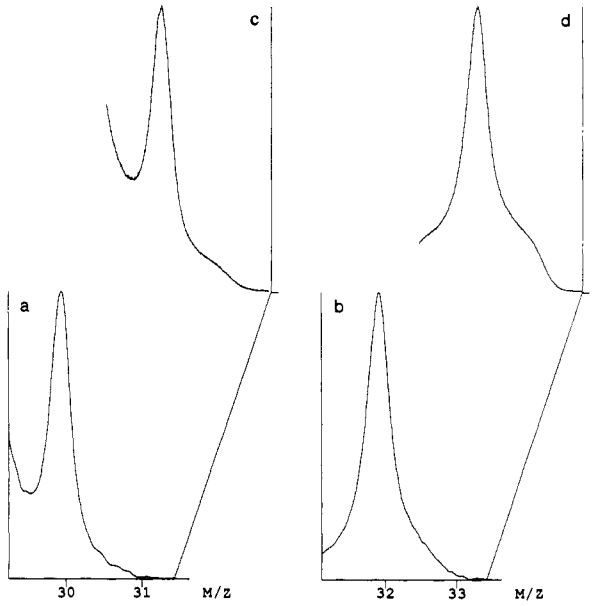

Figure 8. Scan over the peak of (a,c) m/z 30 from $\mathbf{1}^{\bullet+}$ and (b,d) m/z 32 from d_6-$\mathbf{1}^{\bullet+}$, obtained with (a,b) O_2 and (c,d) Xe in the neutralization region. The reionization target is O_2 in all four cases. See text referring to eq 2 for details.

the $^+NR^+$ spectrum is consistent with preservation of the original structure upon neutralization–reionization. The small differences in the abundances of m/z 12–30 between the CAD and $^+NR^+$ spectra of $\mathbf{2}^{\bullet+}$ can be attributed to some CAD taking place, besides neutralization, upon collision of $\mathbf{2}^{\bullet+}$ with Xe. The neutral CAD fragments (mainly $CH_{0-2}O$ according to Figure 4c) produce, after reionization, ions between m/z 12–30; the same ions can also result from surviving **2**. This overlap leads to slightly different relative abundances in the CAD and $^+NR^+$ spectra.

Characterization of Surviving 1. As mentioned above, the weak peaks above m/z 30 and 32 in the $^+NR^+$ spectra of $\mathbf{1}^{\bullet+}$ and d_6-$\mathbf{1}^{\bullet+}$, respectively, indicate that a small fraction of the diradical escapes decomposition to ethylene and formaldehyde. Since these neutral dissociation products can only contribute to the abundances of the $^+NR^+$ peaks up to m/z 30 for **1** and 32 for d_6-**1**, the heavier fragment ions can be used to assess the structure of the survival ion and, thus, the stability of the diradical.

EI of 1,4-dioxane produces a small $C_3H_5O^+$ ion of m/z 57,[37] whose ^{13}C isotope is isobaric with $\mathbf{1}^{\bullet+}$, contributing ~0.8% to the abundance of m/z 58. This contamination cannot be the source of the recovery peak of **1** (Figure 6a) because a comparable recovery ion is observed for the perdeuterated sample (Figure 6b), in which the ^{13}C isotope of $C_3D_5O^+$ (m/z 63) does not overlap with d_6-$\mathbf{1}^{\bullet+}$ (m/z 64). The insensitivity of the relative abundances in the MI spectrum of ion $\mathbf{1}^{\bullet+}$ toward ionizing energy (viz. Figures 1a and 1c) also excludes that the $C_3H_6O^{\bullet+}$ precursor ion beam from 1,4-dioxane contains other isomers. It should be mentioned at this point that the $C_3H_6O^{\bullet+}$ ion from dioxane has been extensively studied by ion–molecule reactions for over a decade and found to contain solely ion $\mathbf{1}^{\bullet+}$.[15,19,20] The photoionization efficiency curve and the appearance energy for $\mathbf{1}^{\bullet+}$ are also incompatible with the presence of other isomers in ion $\mathbf{1}^{\bullet+}$.[16] Contamination is, therefore, unlikely, and the recovered parent ions and heavier fragments in Figures 6a and 6b should originate from the small fraction of neutralized $\mathbf{1}^{\bullet+}$ (or d_6-$\mathbf{1}^{\bullet+}$) which has not decomposed. We still have to determine whether these undissociated species retained the diradical structure until reionization or rearranged to some other more stable molecule.

The simplest isomerization of **1** would be cyclization to the thermodynamically more stable, closed-shell molecule **2** (eq 3).[11,32]

(37) McLafferty, F. W.; Stauffer, D. B. *Wiley/NBS Registry of Mass Spectral Data*; Wiley: New York, 1989.

Whether this happens can be monitored from the relative abundances of $C_3H_{0-3}^+$, which are diagnostic for structure $\mathbf{2}^{\bullet+}$ (*vide supra*). Inspection of the m/z 36–39 regions in the CAD

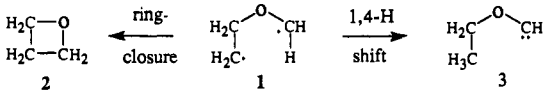

(3)

and $^+NR^+$ spectra of $\mathbf{1}^{\bullet+}$ and $\mathbf{2}^{\bullet+}$ (Figures 4a and 6a vs Figures 4c and 6c) shows that $[C_3H_{0-3}^+]$ remains low for $\mathbf{1}^{\bullet+}$ and does not change markedly upon its $^+NR^+$. Hence, the ring closure **1** → **2** has not occurred to any measurable extent within the ~1-μs time domain available between neutralization and reionization.

Radical sites are prone to intramolecular hydrogen rearrangements. Easiest are H-migrations via five- or six-membered ring transition states. In contrast, H-rearrangements involving three- or four-membered ring intermediates are uncommon because they require much higher activation energies.[38] For example, the isomerization of n-$C_4H_9{\bullet}$ to the more stable[32] sec-$C_4H_9{\bullet}$ via 1,2- or 1,3-H-atom shifts is not observed experimentally.[39] The most facile H-rearrangement for diradical **1** should be the 1,4-hydrogen shift yielding ethoxycarbene, **3** (eq 3). **3** can be produced in the gas phase by neutralization of its stable radical cation, $\mathbf{3}^{\bullet+}$ [14] which is formed upon electron ionization of ethyl glyoxylate (eq 4).[40] The partial CAD and $^+NR^+$ spectra of $\mathbf{3}^{\bullet+}$ illustrated in

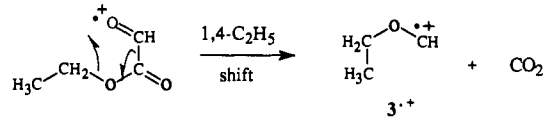

(4)

Figure 9 are distinctively different from the $^+NR^+$ spectrum of $\mathbf{1}^{\bullet+}$ (Figure 6a) both in the m/z 36–43 and m/z 55–58 regions. These dissimilarities exclude any noticeable isomerization of **1** to **3**. The presence of a survival ion in the $^+NR^+$ spectrum of $\mathbf{3}^{\bullet+}$ and of fragments parallel to those formed upon CAD of this ion suggest that ethoxycarbene is a bound molecule.

Since the 1,4-H rearrangement **1** → **3** is not observed, it is improbable that **1** undergoes any other H-migrations in the time window between neutralization and reionization. If undissociated **1** indeed maintains its structure, one would expect that its reionization regenerates $\mathbf{1}^{\bullet+}$ which should yield similar fragments to those observed in the CAD spectrum of $\mathbf{1}^{\bullet+}$. Some products formed upon CAD of $\mathbf{1}^{\bullet+}$ are, however, much less intense or even absent in the $^+NR^+$ spectrum. This can best be seen for d_6-$\mathbf{1}^{\bullet+}$: the expanded traces in Figures 4b and 6b show that after $^+NR^+$, the dissociations $C_2D_5^+ + {\bullet}CDO$ and $^+CD_2OD + C_2D_3{\bullet}$ (both yielding m/z 34), $C_2D_6^{\bullet+} + CO$ (m/z 36), $C_2D_3O^+ + {\bullet}CD_3$ (m/z 46), $C_2D_4O^{\bullet+} + CD_2$ (m/z 48), and $C_3D_5O^+ + {\bullet}D$ (m/z 62) are discriminated against the decompositions producing the other fragments between m/z 33 and 63. Our CAD data of $\mathbf{1}^{\bullet+}$ (Figures 4a and 5) and the energy-resolved CAD study of Verma et al.[17] found the aforementioned reactions to be strongly dependent on the internal energy of the distonic ion $\mathbf{1}^{\bullet+}$ (*vide supra*). Except for the CD_2 loss, all these reactions require complicated isomerizations, and it is possible that collisional reionization produces $\mathbf{1}^{\bullet+}$ in a high internal energy range which does not allow slow, multistep rearrangement fragmentations to compete effectively. Such a phenomenon has been observed previously, e.g., Burgers et al. reported that $CH_3NH{=}NH^+$ ions form abundant $^+NH_4$ (HCN loss) upon CAD but not upon $^+NR^+$.[42] The lack of CH_2 (or CD_2) loss after $^+NR^+$ of $\mathbf{1}^{\bullet+}$ can also be ascribed to internal

(38) Reference 1a, pp 90–97.

(39) Rudat, M. A.; McEwen, C. N. *J. Am. Chem. Soc.* **1981**, *103*, 4349–4354.

(40) Ionized hydroxymethylcarbene ($CH_3COH^{\bullet+}$) and methoxycarbene ($HCOCH_3^{\bullet+}$) have been generated similarly from pyruvic acid[41] and methyl glyoxylate,[31] respectively.

(41) Terlouw, J. K.; Wetzenberg, J.; Burgers, P. C. *J. Chem. Soc., Chem. Commun.* **1983**, *1121*–1123.

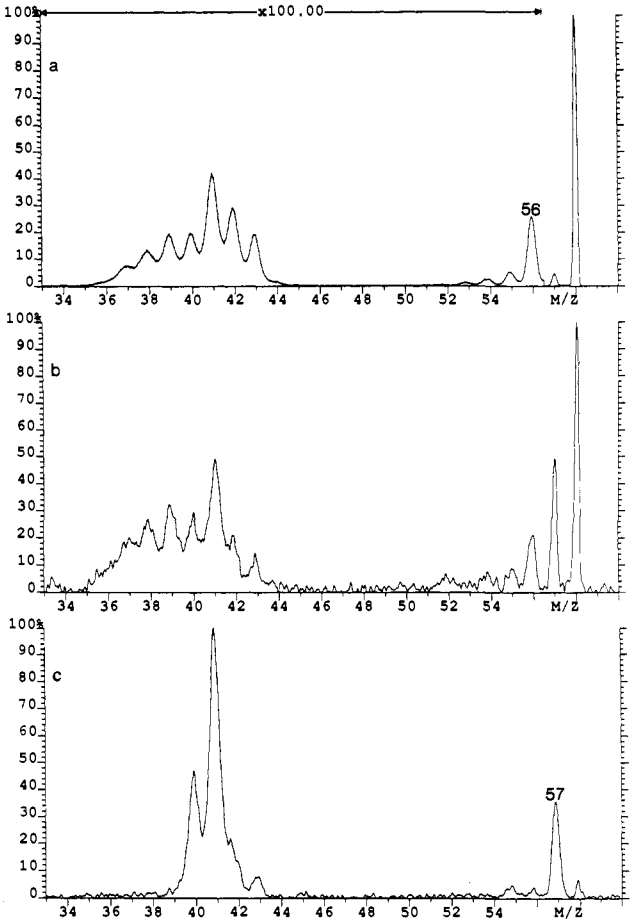

Figure 9. Partial (a) CAD, (b) $^+NR^+$ Xe/O_2, and (c) $^+NR^-$ Xe spectra of ionized ethoxycarbene ($3^{\cdot+}$). The MI spectrum of $3^{\cdot+}$ consists of $C_3H_5O^+$ (100%) and $C_2H_6^{\cdot+}$ (1%).

energy effects. The energy dependence of this cleavage upon CAD suggests that it proceeds from an excited electronic state of $1^{\cdot+}$ (*vide supra*). Apparently, this state cannot be accessed by collisional reionization.[43]

Although the $^+NR^+$ spectrum of $1^{\cdot+}$ clearly shows that diradical **1** has not undergone ring closure to **2** and 1,4-H rearrangement to **3**, it does not provide a straightforward proof for the stability of **1** due to the discussed energy effects, which cause differences between the $^+NR^+$ spectrum and the reference CAD spectrum. Corroborative evidence that neutralization of $1^{\cdot+}$ leads to a species of low ionization energy and with unpaired electrons is provided by producing **1** with a different neutralization target and by reionization into anions.

Neutralization by Trimethylamine. On the basis of the ionization energies (IE) of **1** (6.93 eV)[44] and **2** (9.67 eV),[32] charge exchange with Xe (IE = 12.13 eV)[32] is endothermic for cations $1^{\cdot+}$ and $2^{\cdot+}$, by ~5.2 and ~2.5 eV, respectively.[45] The missing energy in such cases is supplied by the kinetic energy of the precursor ion.[5] The endothermicities can be decreased or even reversed by neutralizing with trimethylamine (TMA), whose

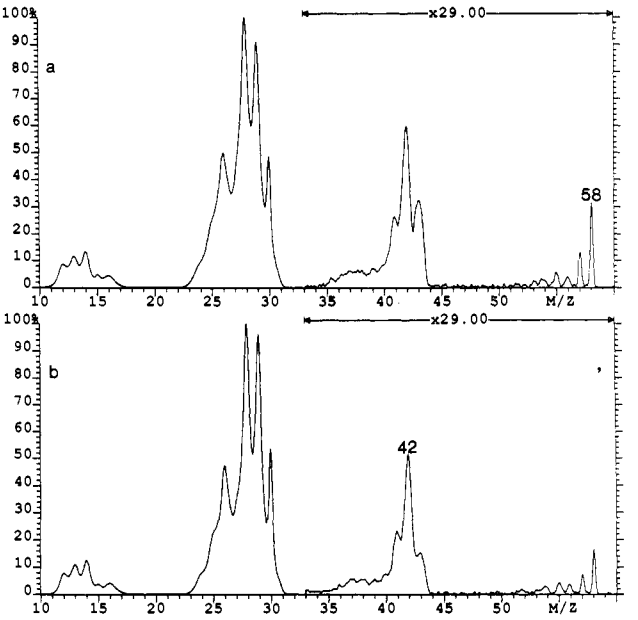

Figure 10. $^+NR^+$ N/O_2 spectra of $1^{\cdot+}$, using as neutralization target N (a) trimethylamine and (b) Xe. The spectra of Figures 6a and 10b were taken 6 weeks apart and illustrate the reproducibility over a longer time period.

vertical IE is 8.44 eV.[46] The reaction $1^{\cdot+}$ + TMA → **1** + $TMA^{\cdot+}$ remains endothermic, although now by a much smaller amount (ΔIE = 1.5 eV), while $2^{\cdot+}$ + TMA → **2** + $TMA^{\cdot+}$ becomes exothermic by ΔIE = −1.2 eV. The excess energy in the latter case is distributed between the two products.[5,6,34]

No visible change occurs in the $^+NR^+$ spectrum of $2^{\cdot+}$ if TMA is used instead of Xe. This is in keeping with the reported decomposition threshold of **2** (2.7 eV),[11] which is much larger than the <1.2 eV available from the exothermic charge exchange. For the $^+NR^+$ spectrum of isomer $1^{\cdot+}$, on the other hand, small changes are observed (Figure 10). With TMA, the relative abundance of the wide peaks between m/z 24–30 increases (as reflected by the shallower valleys between the peaks). This means that collisions with TMA raise the *relative* yield of dissociative neutralization (eq 2b) vs that of CAD (eq 2a). (As explained above, the former process gives rise to the wide and the latter to the narrow components of m/z 24–30.) Changes also occur in the region m/z 33–58, which originates from the surviving fraction of **1**: replacement of Xe by TMA increases the ratio [m/z 36–58]:[m/z 12–30] by ~40% and the relative abundance of the survival ion by ~80% (Figure 10). Overall, more $1^{\cdot+}$ is neutralized and more **1** is produced below its dissociation threshold with TMA than with Xe. Higher charge-exchange cross sections result if the neutralization reaction becomes closer to thermoneutral.[6,47] Hence, the larger yield of **1** with the target of lower ionization energy agrees with the generation of a species of low IE, such as the diradical **1**, upon neutralization of $1^{\cdot+}$.

$C_3H_6O^{\cdot-}$ Radical Anions. The appearance of a small but measurable molecular anion in the $^+NR^-$ spectra of $1^{\cdot+}$ *and* d_6-$1^{\cdot+}$ (Figure 7a) is a further indication that diradical **1** survives partly intact. The closed-shell isomer **2** does not form any bound anion (Figure 7b). The $C_3H_6O^{\cdot-}$ anion in Figure 7a cannot be due to the presence, through isomerization or admixture, of the carbene **3** because the $^+NR^-$ spectrum of the latter (Figure 9c) contains a distinctive peak at m/z 57 that is absent in Figure 7a. Since $\cdot CH_2OCH_2\cdot$ and $\cdot CH_2OH$ have been found to be incapable

(42) Burgers, P. C.; Drewello, T.; Schwarz, H.; Terlouw, J. K. *Int. J. Mass Spectrom. Ion Processes* **1989**, *95*, 157–169.

(43) A related situation is encountered with charge-stripping products. We find that CAD leads to more abundant doubly-charged ions than $^+NR^+$ does. For example, $[CF_3^{++}] + [CF_2^{++}]$ (relative to total fragment ion current) is ~1% in the CAD spectrum of CF_3^+ but only ≤0.1% in the corresponding $^+NR^+$ spectrum (unpublished results from this laboratory).

(44) From $\Delta H°_f(1^{\cdot+}) - \Delta H°_f(1) = 828^{16} - 159^{11} = 669$ kJ mol^{-1} = 6.93 eV. The value of $\Delta H°_f(1)$ is an estimate.[11]

(45) In order to calculate the exact reaction enthalpies for charge exchange, the *vertical* recombination energies of ions $1^{\cdot+}$ and $2^{\cdot+}$ must be known. These are not available, however. Approximate values can be obtained by using the ionization energies of **1** and **2**.

(46) Kimura, K.; Katsumata, S.; Achiba, Y.; Yamazaki, T.; Iwata, S. *Handbook of HeI Photoelectron Spectra of Fundamental Organic Molecules*; Halsted Press: New York, 1981; p 121.

(47) Hop, C. E. C. A.; Holmes, J. L. *Org. Mass Spectrom.* **1991**, *26*, 476–480.

of producing stable anions,[8c,24a] the most likely structure of $1^{\bullet-}$ is $^{-}CH_2CH_2OCH_2^{\bullet}$, which represents a β-O-substituted ethyl anion.

Anion $1^{\bullet-}$ generates $C_2H_3O^-$ (of m/z 43) and CH_3O^- (of m/z 31) fragments via rearrangement cleavages at either side of the ether bond. The former fragment is much less important and the latter absent in the spectrum of anion $2^{\bullet-}$. Note, however, the presence of $C_3H_{0-3}^-$ in the spectrum of $2^{\bullet-}$, which are characteristic for a structure containing three adjacent carbon atoms. Almost all direct cleavages in $1^{\bullet-}$ and $2^{\bullet-}$ initially yield unstable anions (e.g., $C_2H_4^{\bullet-}$ and $OCH_2^{\bullet-}$) which dissociate further giving rise to the lighter fragments in the $^{+}NR^{-}$ spectra (viz. $O^{\bullet-}$, $C_2^{\bullet-}$, C_2H^-, $C_2H_3^-$, and ^{-}OCH).[48]

The major primary decompositions of $1^{\bullet-}$, namely those producing $C_2H_3O^-$ (m/z 43) + $\cdot CH_3$ and $C_2H_3^{\bullet}$ + $^{-}OCH_3$ (m/z 31), proceed via rearrangement. Thus, this stable $C_3H_6O^{\bullet-}$ radical anion resembles the corresponding radical cation in preferring unimolecular dissociations accompanied by isomerization instead of simple bond ruptures. Also, some of the heavier fragments from unstable $2^{\bullet-}$, specifically $C_3H_3O^-$ (m/z 55) and $C_2H_3O^-$ (m/z 43), most probably arise by simple rearrangements.

Conclusions

The main findings of this study can be summarized as follows. (1) The diradical $\cdot CH_2CH_2OCH_2\cdot$ (**1**), which is a proposed intermediate in the thermal decomposition of oxetane (**2**), can directly be accessed in the gas phase by reduction of the distonic radical cation $\cdot CH_2CH_2OCH_2^{+}$ ($1^{\bullet+}$). Once formed, this diradical extensively dissociates by simple bond cleavage yielding $CH_2{=}CH_2$ + $O{=}CH_2$. (2) A small fraction of **1** remains undissociated. Within the microsecond time frame, this fraction neither ring closes to **2** nor undergoes isomerizations involving H-rearrangements. (3) In sharp contrast to diradical **1**, the distonic radical cation $1^{\bullet+}$ decomposes at threshold via complex rearrangements, mainly to $CH_3CH_2C{\equiv}O^+$ + $\cdot H$. Two other important decomposition channels, namely formation of $CH_3C{\equiv}O^+$ + $\cdot CH_3$ and $CH_3CH_3^{\bullet+}$ + CO, also involve rearrangement. (4) The extent of these rearrangement fragmentations is smaller in the $^{+}NR^{+}$ spectrum of $1^{\bullet+}$ than in its CAD spectrum. This could be the result of the deposition of higher internal energies upon collisional reionization than upon CAD. (5) The distonic radical anion $1^{\bullet-}$ is bound, while the closed-shell isomer $2^{\bullet-}$ is not. Several primary decompositions of these $C_3H_6O^{\bullet-}$ anions proceed through rearrangements, thus paralleling those of the $C_3H_6O^{\bullet+}$ radical cations. (6) The MI, CAD, $^{+}NR^{+}$, and $^{+}NR^{-}$ spectra of ions $1^{\bullet+}$ and $2^{\bullet+}$ are substantially different from each other and, thus, consistent with the existence of two distinct radical cations that do not readily equilibrate. This result fully agrees with the distinctive ion–molecule reactions of ions $1^{\bullet+}$ and $2^{\bullet+}$ reported by Kenttämaa et al.[20,22] (7) Our NRMS results describe *qualitatively* the unimolecular chemistry of diradical **1**. Whether the surviving portion is a singlet or triplet state cannot be answered by the experimental data. High-level theoretical calculations could shed more light on this matter as well as provide information on the geometry of **1** and *quantitative* data on the activation energies associated with its unimolecular reactions.

Acknowledgment. The authors are grateful to Christine Miles from Hoechst Celanese Corp. for supplying a sample of ethyl glyoxylate and to John J. Houser for helpful discussions. The National Institutes of Health, the donors of the Petroleum Research Fund, administered by the American Chemical Society, and The University of Akron are thanked for generous financial support.

(48) The dissociating fraction of **1** yields $CH_2{=}CH_2$ and $O{=}CH_2$. These closed-shell molecules have large cationization but poor anionization efficiencies. For example, pure $CH_2{=}CH_2^{\bullet+}$ produces ~10 times more cations upon $^{+}NR^{+}$ and ~2 times less anions upon $^{+}NR^{-}$ (at 3.8 keV) than an equivalent amount of $1^{\bullet+}$ (at 8.0 keV). Consequently, the decomposition products of **1** are visible in the $^{+}NR^{+}$ spectrum of $1^{\bullet+}$ but do not contribute appreciably to its $^{+}NR^{-}$ spectrum.